



**FACULTY OF ELECTRICAL ENGINEERING
AND INFORMATION SCIENCE**



**INFORMATION TECHNOLOGY AND
ELECTRICAL ENGINEERING -
DEVICES AND SYSTEMS,
MATERIALS AND TECHNOLOGIES
FOR THE FUTURE**

Startseite / Index:

<http://www.db-thueringen.de/servlets/DocumentServlet?id=12391>

Impressum

Herausgeber: Der Rektor der Technischen Universität Ilmenau
Univ.-Prof. Dr. rer. nat. habil. Peter Scharff

Redaktion: Referat Marketing und Studentische
Angelegenheiten
Andrea Schneider

Fakultät für Elektrotechnik und Informationstechnik
Susanne Jakob
Dipl.-Ing. Helge Drumm

Redaktionsschluss: 07. Juli 2006

Technische Realisierung (CD-Rom-Ausgabe):
Institut für Medientechnik an der TU Ilmenau
Dipl.-Ing. Christian Weigel
Dipl.-Ing. Marco Albrecht
Dipl.-Ing. Helge Drumm

Technische Realisierung (Online-Ausgabe):
Universitätsbibliothek Ilmenau
[ilmedia](#)
Postfach 10 05 65
98684 Ilmenau

Verlag:  Verlag ISLE, Betriebsstätte des ISLE e.V.
Werner-von-Siemens-Str. 16
98693 Ilmenau

© Technische Universität Ilmenau (Thür.) 2006

Diese Publikationen und alle in ihr enthaltenen Beiträge und Abbildungen sind urheberrechtlich geschützt. Mit Ausnahme der gesetzlich zugelassenen Fälle ist eine Verwertung ohne Einwilligung der Redaktion strafbar.

ISBN (Druckausgabe): 3-938843-15-2
ISBN (CD-Rom-Ausgabe): 3-938843-16-0

Startseite / Index:
<http://www.db-thueringen.de/servlets/DocumentServlet?id=12391>

M. Schühler, C. Schmidt, J. Weber, R. Wansch, and M. A. Hein

Phase Shifters based on PIN-Diodes and Varactors: Two Concepts by Comparison

ABSTRACT

The emphasis of this paper is on the comparison between two diode-based phase shifters. First, a 4-bit 360° switched-line phase shifter is manufactured using pin-diodes as switching devices. Thereafter, a 360° hybrid-coupled reflection-type phase shifter is implemented using varactor diodes as variable reactances. It will be shown that the hybrid-coupled phase shifter is a good alternative to the switched-line phase shifter. The comparison of the two investigated phase shifters considers typical criteria like control power, quality factor and third order intercept point among others. The examinations were performed in the 2.4-GHz ISM-Band.

I. INTRODUCTION

Modern radio communication systems should provide optimal transmitting and receiving properties for an improved utilisation of transmission channels. Focussing on the antennas, this requires electronically steerable radio patterns, which can be achieved using phased array antennas. A fundamental part of phased array antennas are the phase shifters. The phase shifters determine the differential signal phase shift of each antenna or antenna subgroup.

Phase shifters based on diodes are well known in literature. One of the most important is the “switched-line phase shifter” [1], where the phase shift corresponds to the length difference between two switched transmission lines. The switching procedure is obtained by changing the bias point of a pin-diode from forward to reverse direction and vice versa. Using this method, the phase shift can be controlled digitally, hence no digital-to-analog conversion is required.

Another type of phase shifter uses common pn-diodes, which act as variable reactances (varactors). The actual phase shift results from the signal reflection at a varactor terminated transmission line [2]. The separation of the incoming and the reflected signal is provided by a hybrid coupler, hence this type of phase shifter is called “hybrid-coupled reflection-type phase shifter” (HCRT phase shifter).

The paper focusses on the comparison of the two investigated phase shifters in

terms of practical criteria such as control power, phase accuracy, quality factor and third order intercept point. It will be shown that the hybrid-coupled reflection-type phase shifter is an excellent alternative to the switched-line device. At first, the fundamentals and the design processes of the two prepared circuits will be presented followed by the evaluation of the simulation and measurement results.

II. SWITCHED-LINE PHASE SHIFTER

A. Principle

A simplified schematic of a switched-line phase shifter section is shown in Fig. 1 [2]. In switching state “1” the upper path is isolated and the incoming signal passes the

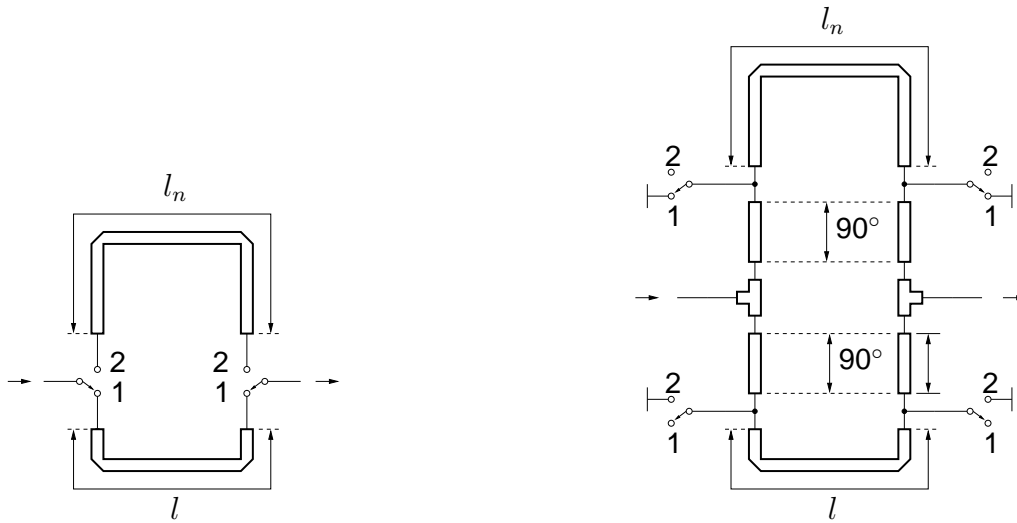


Figure 1: Schematic of the n -th section of a switched-line phase shifter: On the left side the switches are in series, on the right side in shunt configuration. The characteristic wave impedance of the transmission lines is equal to the source and load impedance.

lower transmission line. After changing the switching state to “2” the upper path will be passed and the lower path is isolated. The length difference $\Delta l_n = l_n - l$ of the two paths results in a differential phase shift of the n -th switched-line section, which is given by

$$\psi_n = k_c \Delta l_n . \quad (1)$$

In (1) k_c is the phase propagation constant of the transmission line at the center frequency, f_c .

Due to the finite isolation of switches in practice, the lengths of the transmission lines have to be chosen carefully. In case of electrical lengths of $n\pi$ ($n \in \mathbb{Z}$) resonance effects can occur, which result in a large insertion loss and large phase errors [1]. As recommended by Garver [1], the electrical length of the reference line should be in the range between 20° and 50° to prevent resonance effects. For the prepared switched-line phase shifter l is chosen within this range. Using this length and the desired total

phase shift $\widehat{\Psi}$, the lengths of the transmission lines of a switched-line phase shifter with a resolution of N bit are given by

$$l_n = l + \frac{1}{k_c} \frac{\widehat{\Psi}}{2^{N-n}}, \quad n = 0, 1, \dots, N - 1. \quad (2)$$

B. Implementation

In general, pin-diodes act as single-pole single-throw switches (SPST), so per switched-line section four diodes are required (two at each branching point). If the used diodes¹ are mounted as shunt devices, as shown in the right picture of Fig. 1, the isolation of the off-path is approximately 6 dB larger in contrast to the configuration with series switches (left picture of Fig. 1). Therefore, at the manufactured switched-line phase shifter, the pin-diodes were mounted as shunt switches each coupled by a 90° transmission line to the branching point (see Fig. 2). Note, to dimension this line the phase offset of the forward-biased pin-diode, which is mainly caused by the lead inductance, has to be considered to provide a sufficient transformation between ground and the branching point.

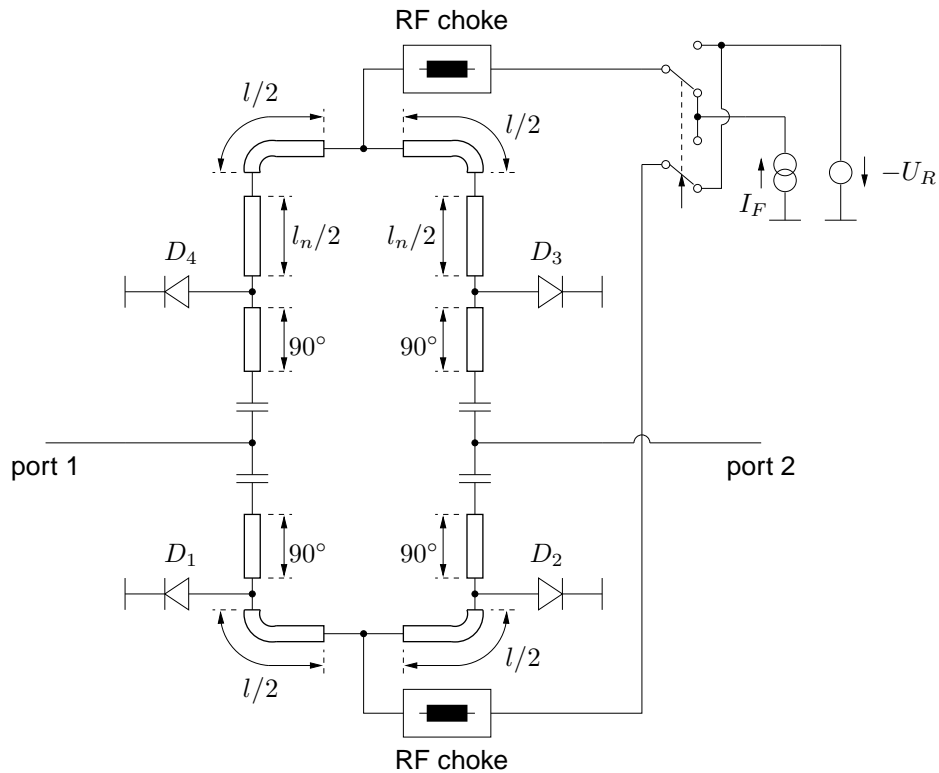


Figure 2: Schematic of a switched-line section using pin-diodes in shunt configuration: If the diodes D_1 and D_2 are forward biased (bias current I_F), then D_3 and D_4 are biased in reverse direction (reverse voltage $U_R \geq 0$) and vice versa. The characteristic wave impedance of the transmission lines is matched to the source and load impedance. The capacities act as DC blocks. The RF chokes decouple the RF signal from the DC source.

¹BAR89 from Infineon

In addition to the RF part, a TTL compatible driver circuit as proposed by White [3] was implemented to bias the pin-diodes. In forward direction, the diodes are fed with a current of 10 mA. In reverse direction, the diodes are biased by a reverse voltage of 5 V. At each switched-line section, two driver circuits are used to bias two diodes in forward and two in reverse direction, respectively. Because a resolution of 4 bit was aimed for the switched-line phase shifter, overall sixteen pin-diodes and, thus, eight drivers are required. To decouple the driver circuits from the RF signal, distributed bandstop filters were implemented.

The switched-line phase shifter was built on a 0.51 mm thick FR-4 substrate with a relative permittivity of $\epsilon_r = 4.34$.

C. Measurement Results

S-Parameters: The scattering parameters of the prepared switched-line phase shifter were taken between 2.30 and 2.60 GHz using a vector network analyser. Fig. 3 shows on the left side the measured phase constellation of the 4-bit switched-line phase shifter at 2.45 GHz. The largest insertion loss of 6.5 dB corresponds to the largest possible

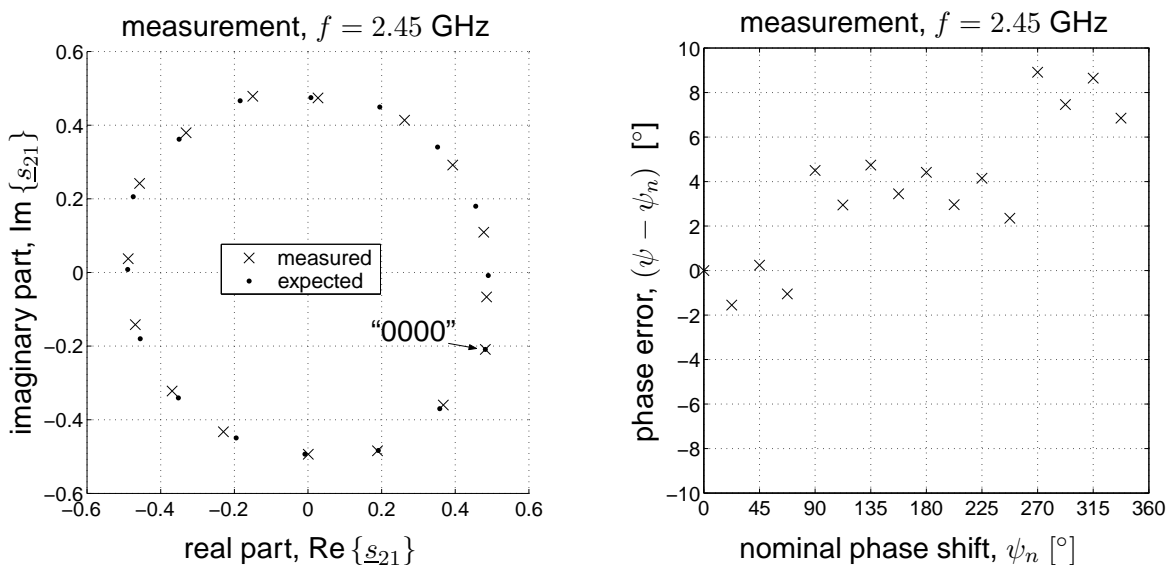


Figure 3: Measured phase constellation (left) and phase error (right) of the switched-line phase shifter at 2.45 GHz; the reference point ($\psi_n = 0^\circ$) is indicated by the binary word "0000".

phase shift, because in this case the signal passes the longest path. The value of 6.5 dB is nearly 2.0 dB larger compared to the foregoing simulation. This is mainly caused by the insufficient short-open transformation, because the lead inductance of the diodes were larger than in the simulation model. Furthermore, a resonance effect was observed in the 90° switched-line section, which could be traced back to the larger inductance as well. At further measurements the resonance was suppressed manually by connecting a 50Ω load to the off-path. Due to the non-ideal short-open transformation the 10-dB matching bandwidth of $(2.46 - 2.42) \text{ GHz} = 40.0 \text{ MHz}$ is quite small in

comparison to the simulation results, where a bandwidth of 1.02 GHz could be reached. In addition, the maximum phase error of 8.9° (see Fig. 3 right) is caused by the insufficient transformation as well. All these effects could be verified by further simulations, where an increased lead inductance was included.

As suggested by (1), for a switched-line phase shifter the phase shift depends linearly on the frequency. The pin-diode phase shifter shows this behaviour only at frequencies close to 2.45 GHz (see Fig. 4 right). Anyway, the group delay variations of

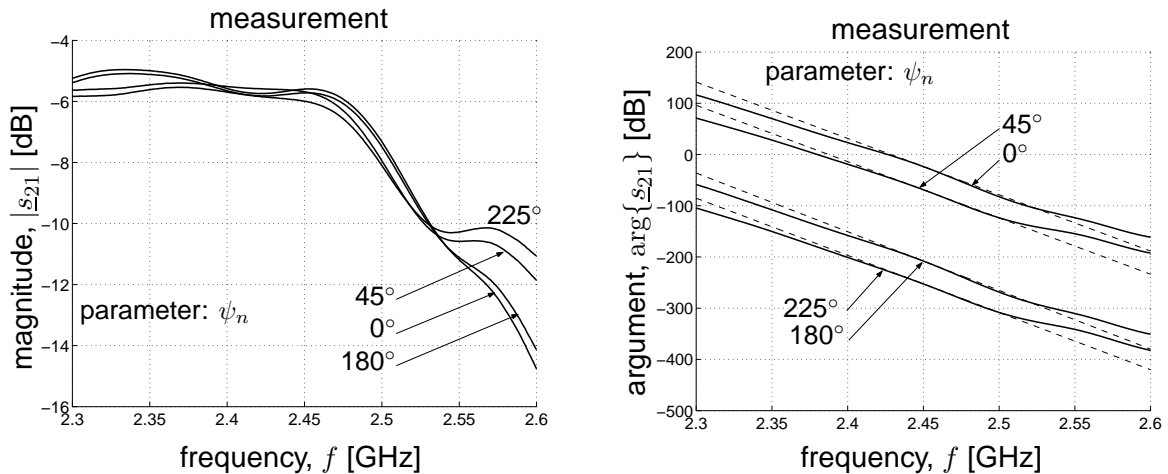


Figure 4: Frequency response of the switched-line phase shifter: On the left side the magnitude, $|s_{21}|$, on the right side the argument, $\arg\{s_{21}\}$, is displayed. Parameter is the nominal phase shift, ψ_n . The dashed lines indicate the tangents at 2.45 GHz.

0.54 ns are small within the frequency band of interest. The frequency response of the magnitude of the forward transmission factor, s_{21} , is shown on the left side of Fig. 4. Looking at the center frequency of 2.45 GHz, the amplitude ripple amounts to 0.9 dB.

Third Order Intercept (TOI): To measure the intermodulation distortions, the phase shifter was fed by a two-tone signal with a frequency offset of 2.0 MHz. The output port of the device was connected to a spectrum analyser. The prepared switched-line phase shifter offers a third order intercept point of 30.8 dBm.

Temperature Dependency: In a further measurement the phase shifter was put into a climatic chamber to find out how the differential phase shift is influenced by the ambient temperature. Fig. 5 shows the measurement result. According to the reference value at 25°C , the maximal drift of the differential phase shift is 1.6° considering a temperature range from -25.0°C to $+50.0^\circ\text{C}$.

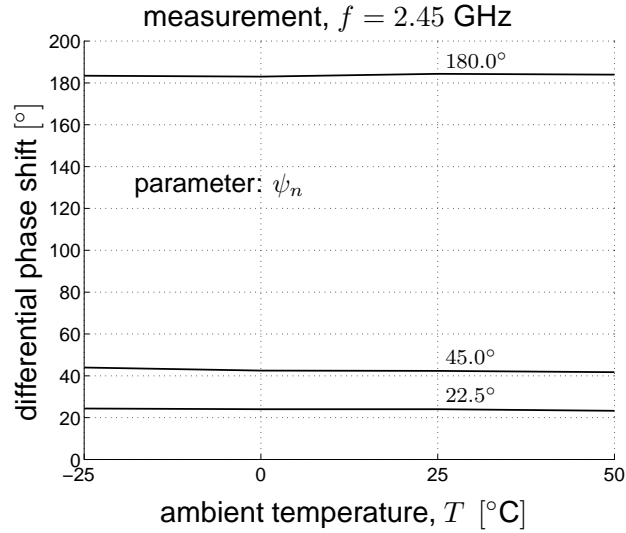


Figure 5: Differential phase shift at 2.45 GHz as a function of ambient temperature, T , for three different nominal phases.

III. HYBRID-COUPLED REFLECTION-TYPE PHASE SHIFTER

A. Principle

A simplified schematic of a HCRT phase shifter shows Fig. 6. The incoming signal is split into two quadrature components with similar magnitude by a 3-dB 90° hybrid coupler. The scattering matrix of the hybrid coupler is defined as

$$\mathbf{S} = -\frac{1}{\sqrt{2}} \begin{bmatrix} 0 & 0 & 1 & j \\ 0 & 0 & j & 1 \\ 1 & j & 0 & 0 \\ j & 1 & 0 & 0 \end{bmatrix}. \quad (3)$$

The outgoing quadrature components at port 3 and 4 are reflected back by the load, which is ideally a pure reactance denoted by X_L , thus the reflection coefficient is given by

$$\underline{\gamma}_L = \frac{X_L - Z_W}{X_L + Z_W}; \quad (4)$$

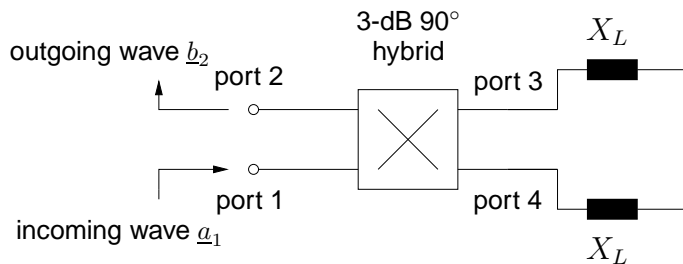


Figure 6: Schematic of the HCRT phase shifter

Z_W is the source and load impedance, respectively. The signal reflections correspond to a phase shift of the quadrature components, which is determined by the argument of $\underline{\gamma}_L$

$$\arg\{\underline{\gamma}_L\} = \pi - 2 \arctan\left(\frac{X_L}{Z_W}\right). \quad (5)$$

The reflected waves add up in-phase at port 2 and out-of-phase at port 1, hence the HCRT phase shifter is matched perfectly. Using (3) and (5), the overall phase shift of the HCRT phase shifter is given by

$$\arg\{\underline{s}_{21}\} = \psi = -\frac{3}{2}\pi + \arg\{\underline{\gamma}_L\} = -\frac{1}{2}\pi - 2 \arctan\left(\frac{X_L}{Z_W}\right). \quad (6)$$

B. Reflective Load

The main item of a HCRT phase shifter is the reflective load, which determines the total phase shift, $\hat{\Psi}$, the amplitude ripple, and the sensitivity, S_ψ (see (11) below). Garver [4], Tamm [5], and Liew [6] describe the design of reflective networks, which offer a 360° total phase shift. The networks use varactor diodes and quarter-wavelength transformers among compensating components.

Looking at the HCRT phase shifter built here, the solution proposed by Garver [4] was implemented as reflective network, which is shown schematically in Fig. 7. Assuming that the diode can be described as a pure reactance denoted by X_d and the

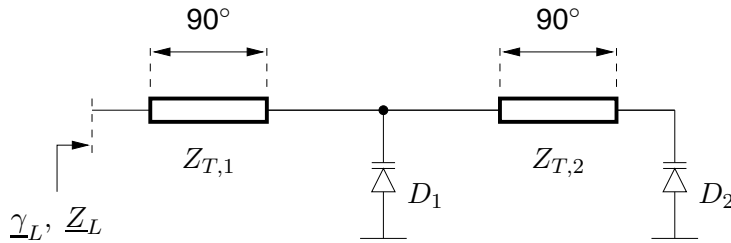


Figure 7: Schematic of the reflective load of the HCRT phase shifter

quarter-wavelength transformers are lossless, the load impedance is only reactive as well; it is given by

$$\underline{Z}_L = j X_L = j \frac{Z_{T,1}^2}{Z_{T,2}^2} \frac{X_d^2 - Z_{T,2}^2}{X_d}, \quad (7)$$

where $Z_{T,1}$ and $Z_{T,2}$ are the characteristic wave impedance of the quarter-wavelength transmission lines. Insert (7) in (5), the argument of $\underline{\gamma}_L$ is

$$\arg\{\underline{\gamma}_L\} = \pi - 2 \arctan\left(\frac{Z_{T,1}^2}{Z_{T,2}^2} \frac{X_d^2 - Z_{T,2}^2}{X_d Z_W}\right). \quad (8)$$

In practice, the reactance of a varactor diode can be written as

$$X_d(U_R) = \omega L_s - \frac{1}{\omega C_d(U_R)}, \quad (9)$$

here L_s is the lead inductance, and C_d stands for the reverse voltage dependent junction capacitance; the capacitances caused by the package geometry are neglected. As denoted in (9), X_d is a function of the reverse voltage, U_R , applied to the varactor diode. By varying the reverse voltage, the junction capacitance is changed, and so is the argument of the reflection coefficient.

To achieve the desired performance of the HCRT phase shifter, the characteristic impedances $Z_{T,1}$ and $Z_{T,2}$ of the quarter-wavelength transformers have to be dimensioned in the right way. They have influences on

- the total phase shift,
- the amplitude ripple,
- the insertion loss,
- and the sensitivity.

To demonstrate how the behaviour of the HCRT phase shifter depends on $Z_{T,1}$ and $Z_{T,2}$, a simulation of the reflective load (see Fig. 7) was accomplished using a model of the varactor diode “BB833”². Within the frequency band of interest, this diode has an inductive reactance at lower reverse voltages due to the lead inductance. By increasing U_R the width of the depletion layer increases and, thus, the junction capacitance decreases. Therefore, at higher reverse voltages the reactance of the varactor diode is capacitive. The left picture of Fig. 8 shows that the total phase shift increases by decreasing $Z_{T,2}$. Typically total phase shifts of more than 360° are not required. Hence, the value of $Z_{T,2}$ should not be chosen lower than necessary, because a too small impedance involves a high insertion loss as can be seen in the right picture of Fig. 8. This is because the small bulk resistance is transferred to a higher value by the quarter-wavelength transformer. Anyway, to obtain a total phase shift of exactly 360° , $Z_{T,2}$ can be calculated using the expression

$$Z_{T,2} = \sqrt{-X_{L,1} X_{L,2}} \quad (10)$$

where $X_{L,1}$ and $X_{L,2}$ describe the diode reactance at zero and maximal reverse voltage, respectively. Note, (10) is only an approximation, because the real part of the diode impedance is not included. However, $Z_{T,2}$ can be well estimated by (10): The value of 36.1Ω determined using (10) is quite close to the result got by the simulation (see Fig. 8), where a total phase shift of 360° is reached for $Z_{T,2} = 37.4 \Omega$.

²from Infineon

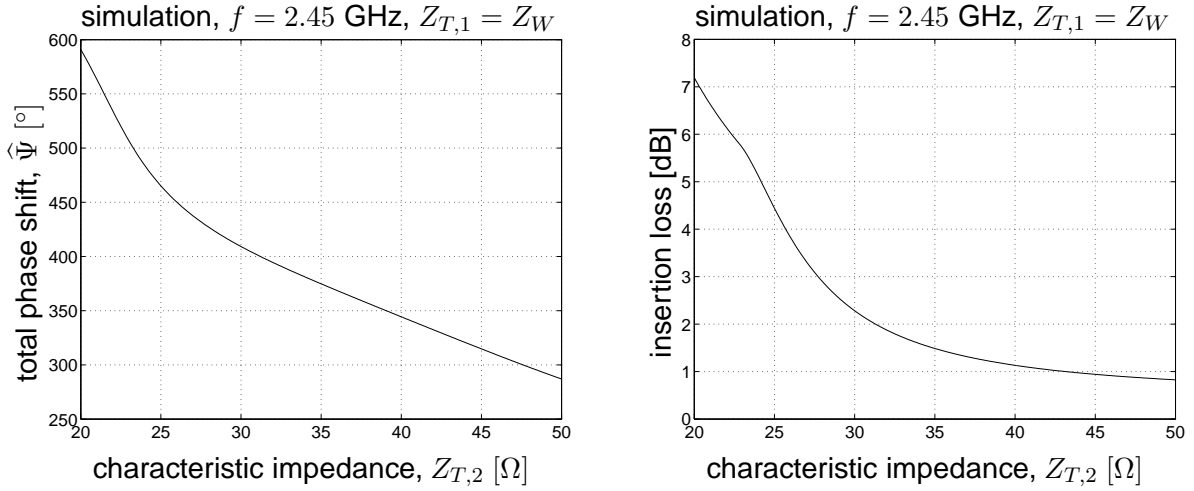


Figure 8: Total phase shift, $\hat{\Psi}$, (left) and insertion loss (right) as a function of $Z_{T,2}$: The simulation was performed at 2.45 GHz looking at the possible range of the reverse voltage.

Note, to get a real characteristic impedance $Z_{T,2}$ from (10), the diode reactance has to switch over from inductive to capacitive behaviour within the possible range of the reverse voltage. That means, a non-zero lead inductance is useful. If the diode reactance is only capacitive (at lower frequencies) or inductive (at higher frequencies), an additional reactive component (typically distributed) is required.

After we have discussed, how the behaviour of the HCRT phase shifter depends on $Z_{T,2}$, now the influence of $Z_{T,1}$ will be considered. On the right side of Fig. 9 it is shown, that both the sensitivity, which is defined as

$$S_\psi = \max_{U_R} \left\{ \frac{d\psi}{dU_R} \right\}, \quad (11)$$

and the amplitude ripple changes with $Z_{T,1}$. As denoted in (11), the sensitivity is the

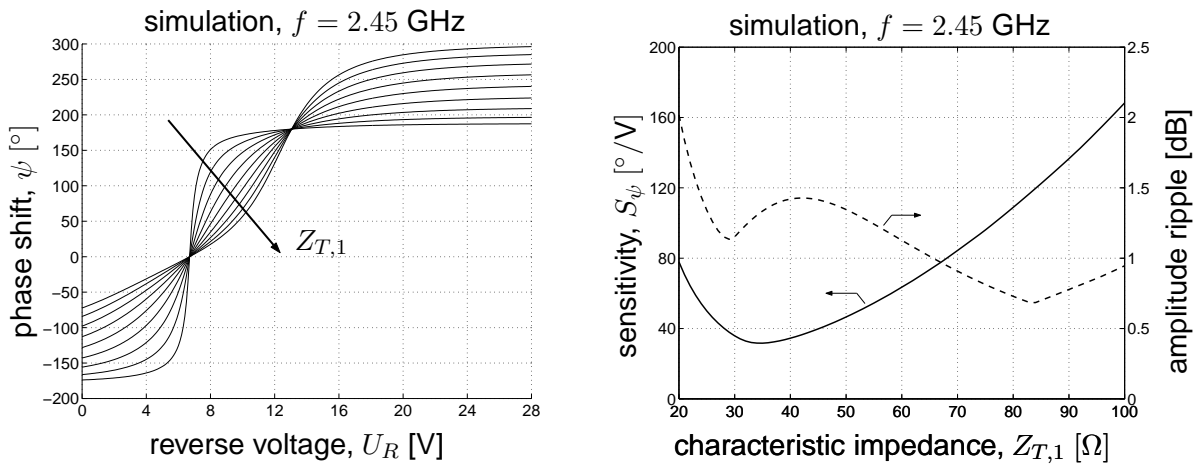


Figure 9: Phase shift, ψ , as a function of U_R for $Z_{T,1} = \{10, 20, 30, 40, 50\} \Omega$ (left) and the sensitivity S_ψ and the amplitude ripple, respectively, as a function of $Z_{T,1}$ (right): The simulation was accomplished using a model of the diode “BB833.” The intersection points in the left plot indicate the resonance points of the reflective network.

maximum of the derivation of the phase shift, ψ , with respect to the reverse voltage, U_R . The smallest sensitivity of $0.03^\circ/\text{mV}$ is reached for $Z_{T,1} = 35.4 \Omega$, but the smallest amplitude ripple of 0.7 dB is attained for $Z_{T,1} = 83.0 \Omega$. Looking at the HCRT phase shifter built up here, $Z_{T,1}$ was optimised with respect to S_ψ , because a small sensitivity involves a large third order intercept point (TOI).

As can be seen in the left picture of Fig. 9, where ψ is displayed as a function of U_R , the total phase shift depends on $Z_{T,1}$ barely — only the gradient is effected by the characteristic impedance of the quarter-wavelength transformer.

C. Implementation

Figure 10 shows the schematic of the prepared HCRT phase shifter. To split the in-

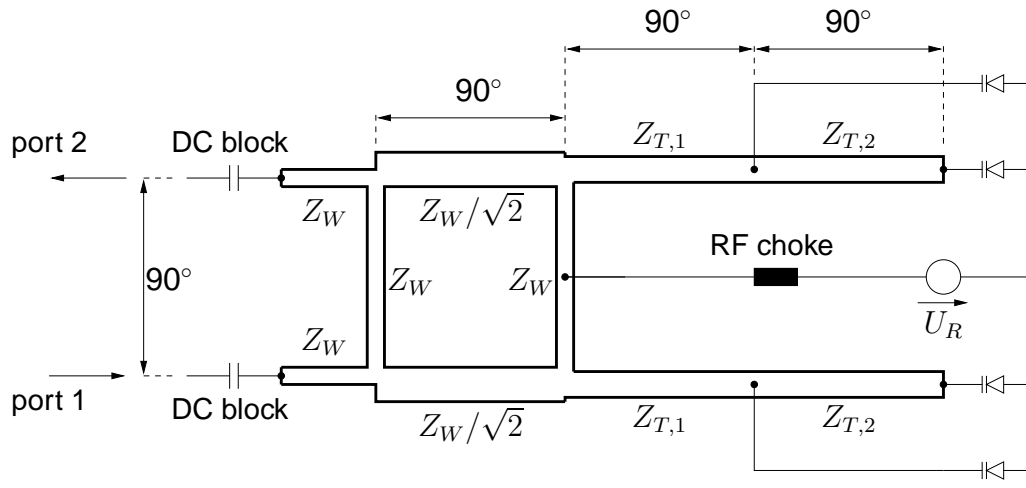


Figure 10: Schematic of the HCRT phase shifter: A branch-line coupler act as 3-dB 90° hybrid. The capacities decouple the RF source and load, respectively, from the DC bias signal applied to the diodes.

coming signal into two quadrature components a 3-dB 90° branch-line coupler was implemented. The characteristic impedance, $Z_{T,2}$, of the second quarter-wavelength transformer was chosen to 35.8Ω to obtain a total phase shift of 370.0° . So the desired phase shift of 360.0° can be obtained even in case of inaccuracies in fabrication.

The bias voltage is fed over a surface-mount chip inductor, whose resonance frequency is nearly 3.0 GHz and, thus, above the frequency band of interest.

As the switched-line phase shifter (see Section II.B.), the HCRT phase shifter was built on a 0.51 mm thick FR-4 substrate.

D. Measurement Results

S-Parameters: As for the switched-line phase shifter the scattering parameters of the HCRT phase shifter have been taken between 2.30 and 2.60 GHz using a vector network analyser. The phase constellation and the argument of the forward transmission

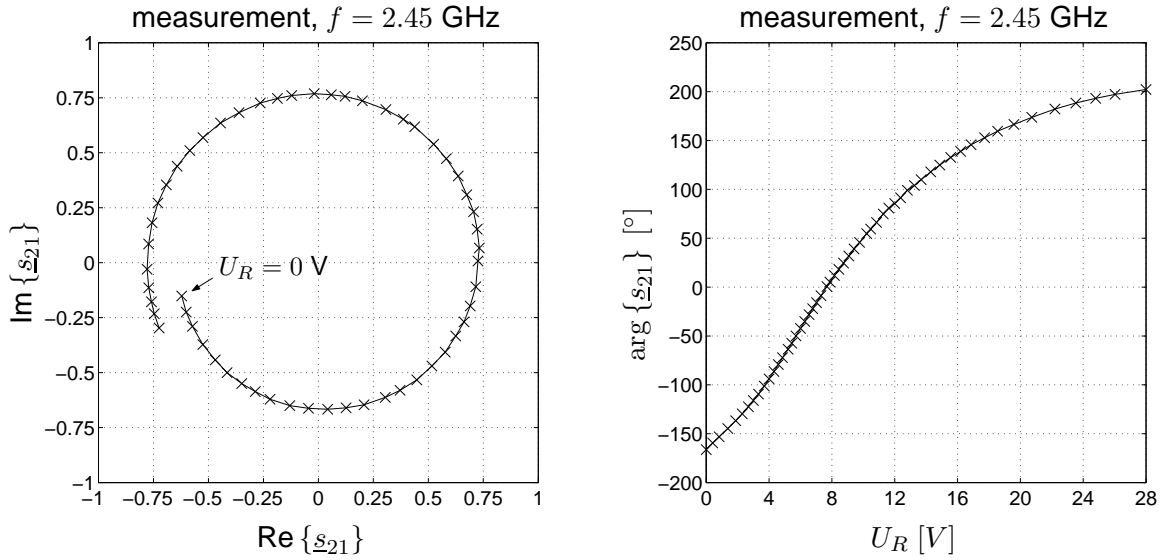


Figure 11: Measurement results of the HCRT phase shifter at 2.45 GHz: In the left picture the phase constellation is displayed; on the right side the argument of \underline{s}_{21} as a function of reverse voltage, U_R , is shown. There was linear interpolated between the measurement points (cross-marked).

factor, \underline{s}_{21} , are shown in Fig. 11. As can be seen on the left side, the insertion loss varies with the reverse voltage, because besides the junction capacitance the bulk resistance depends also on U_R . At $U_R = 0$ V, the insertion loss reaches a maximum of 3.8 dB. By increasing U_R the depletion layer of the varactors extends more and more into the bulk regions. Therefore, the width of the bulk region and, thus, the bulk resistance decreases, and so is the insertion loss. For $U_R = 28$ V the HCRT phase shifter exhibits the slightest insertion loss of 2.0 dB.

By varying the reverse voltage of the diodes within the possible range from 0 to 28 V, the signal phase can be steered about 368.6° (see Fig. 11 right). A value of 360° is already reached at $U_R = 25.0$ V. The sensitivity amounts to approximately $0.03^\circ/\text{mV}$.

Within the frequency band of interest, the argument of \underline{s}_{21} falls nearly linear with frequency, as can be seen in Fig. 12 right. Hence the average group delay fluctuations of 0.51 ns are quite small. The frequency response of the magnitude, $|\underline{s}_{21}|$, is especially influenced by the hybrid coupler and the quarter-wavelength transformers. Assuming a constant reverse voltage, the amplitude ripple with respect to frequency is ≤ 0.4 dB within the considered ISM band (see Fig. 12 left).

Regarding to the input reflection factor, \underline{s}_{11} , a 10-dB matching bandwidth of (2.80 – 2.12) GHz = 0.68 GHz is achieved. This value is 0.16 GHz larger compared to the result of the foregoing simulation. Looking at the center frequency of 2.45 GHz, the magnitude of \underline{s}_{11} does not exceed a value of 0.11 (-19.2 dB) about the valid reverse voltage range.

Third Order Intercept: The measurement of the intermodulation distortions was performed using a spectrum analyser. As in the case of the switched-line phase shifter, the

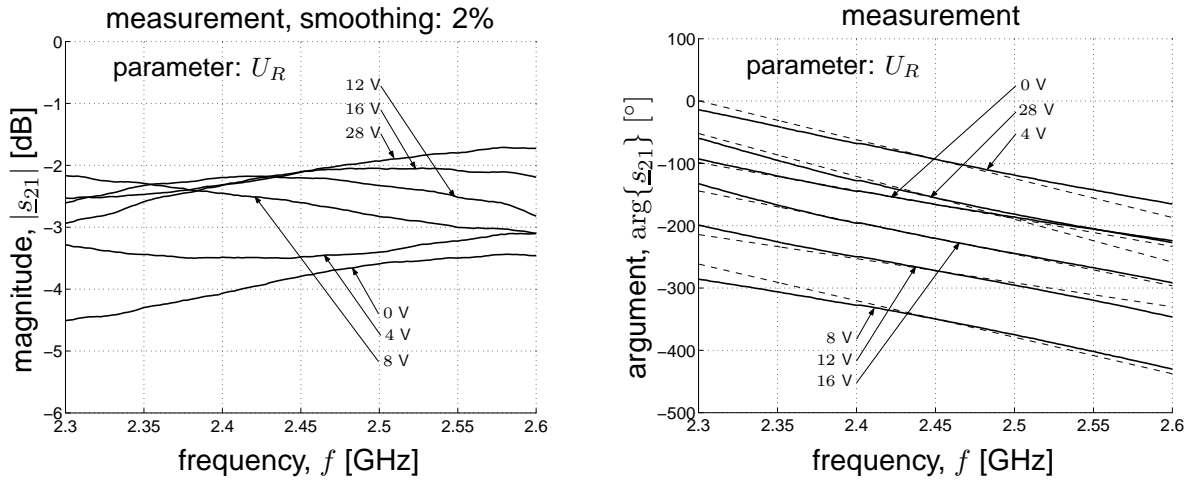


Figure 12: Frequency response of the HCRT phase shifter: The left picture shows the magnitude, the right one the argument; in both plots the reverse voltage, U_R , was varied. The non-linear relationship between the argument and frequency, which is given by (6) using (7) and (9), is especially distinct at frequencies far away from the center frequency of 2.45 GHz. This is stressed by the tangents at 2.45 GHz (dashed lines).

HCRT phase shifter was fed by an two-tone signal with a frequency offset of 2.0 MHz. Because of the non-linear relationship between the phase shift and the reverse voltage (see Fig. 11 right), the TOI depends on the bias state of the varactors. The largest distortions occur in the region, where the ψ - U_R -diagram shows the maximal gradient. At this point the TOI of the HCRT phase shifter amounts to 27.9 dBm.

Temperature Dependency: The prepared HCRT phase shifter was also characterised in a temperature-variant environment. Fig. 13 shows the measured differential phase shift as a function of ambient temperature for different reverse voltages. Considering a temperature range from -25.0°C to $+50.0^\circ\text{C}$, the maximal drift of the differential phase shift is 4.0° related to the reference measurement at $T = 25.0^\circ\text{C}$.

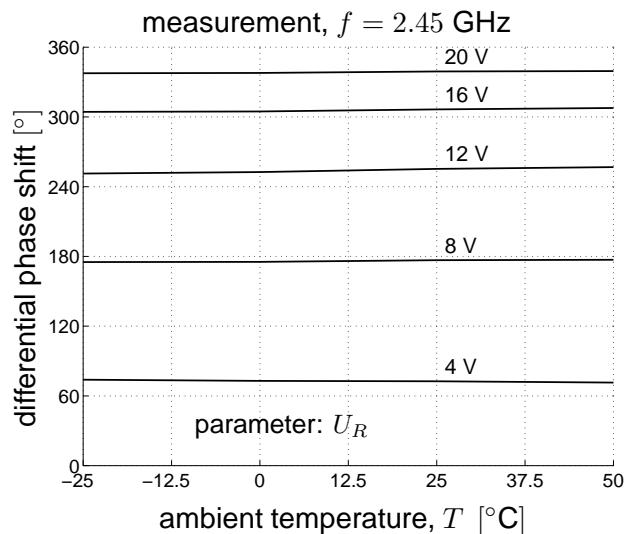


Figure 13: Differential phase shift at 2.45 GHz as a function of ambient temperature, T , for five different reverse voltages, U_R

IV. COMPARISON

In general, with phase shifters both a small insertion loss and a small input reflection is aspired independent of the implemented concept. Furthermore the total phase shift, the phase error, and the phase resolution are important parameters of phase shifters. An important comparable characteristic of phase shifters is the quality factor, Q_ψ , which is defined as the maximum phase shift over insertion loss [2]. Fig. 14 shows the frequency response of Q_ψ for the two investigated phase shifters. As can be seen in the

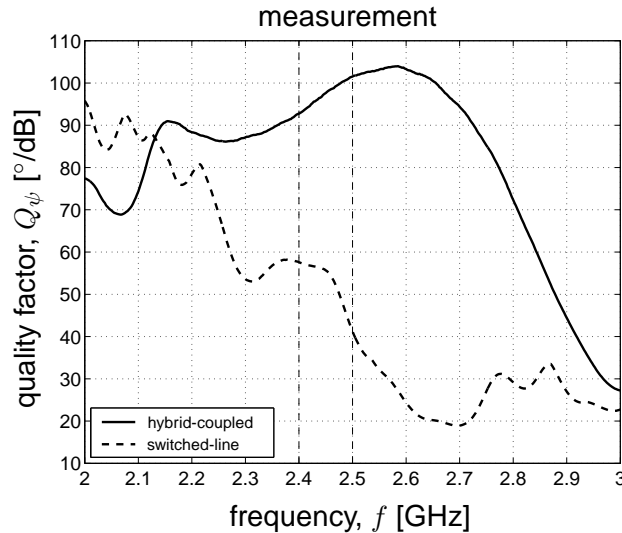


Figure 14: Measured frequency response of the quality factor, Q_ψ : The dashed vertical lines indicate the frequency band of interest.

plot, within the frequency band of interest, the HCRT phase shifter offers a much larger quality factor compared to the switched-line device. Primarily this can be attributed to a lower insertion loss.

In Table 1 the results of the two manufactured phase shifters are shown. Besides the above mentioned parameters, the amplitude ripple at 2.45 GHz considering all phase states, the 10-dB matching bandwidth, the TOI, the group delay variations within the frequency band of interest, the temperature drift of the differential phase shift at 2.45 GHz, and the required control power are also listed.

For the HCRT phase shifter no phase error can be noted: If the relationship between the phase shift and the reverse voltage known, the phase shift can be steered with arbitrary precision. The precision of the switched-line phase shifter is limited by the area constraints of the circuit, because by increasing the phase resolution the occupied area increases as well. Anyway, a large phase resolution means small phase shifts for the lower significant bits and, thus, high accuracy in fabrication of these switched-line sections is required. Due to the reverse biased varactor diodes the required control power of the HCRT phase shifter is quite small. On the other hand, in contrast to the switched-line phase shifter, the amplitude ripple of the HCRT device is larger. This is caused by the bulk resistance, which varies with the applied reverse voltage. However,

comparable criteria	switched-line phase shifter using pin-diodes	HCRT phase shifter using varactor diodes
total phase shift, $\hat{\Psi}$ [°]	360	368.6
phase error [°]	8.9	—
resolution [Bit]	4	arbitrary
temperature drift [°]	± 1.6	± 4.0
insertion loss [dB]	6.5	3.8
amplitude ripple [dB]	0.9	1.8
maximal input reflection [dB]	-12.6	-19.2
10-dB matching bandwidth [GHz]	0.04	0.68
quality factor, Q_ψ [°/dB]	55.4	97.0
TOI [dBm]	30.8	27.9
group delay variations [ns]	0.54	0.51
control power [mW]	66.4	≤ 0.02

Table 1: Comparison of the two investigated phase shifters: Except for the 10-dB matching bandwidth, the TOI, and the group delay variations, all values are taken at the center frequency of 2.45 GHz. In the case of the switched-line phase shifter, the control power was calculated without including the small reverse current of the pin-diodes. The forward current of each diode was limited to 10 mA.

by putting a ohmic resistance parallel to the varactor diodes, the amplitude ripple can be decreased [4].

In phased arrays the phase shift is typically controlled by digital signals, therefore the switched-line phase shifter is well suited — using the HCRT phase shifter a digital-analog converter is needed. The switched-line phase shifter has a small 10-dB matching bandwidth compared to the HCRT device. However, this is due to the insufficient short-open transformation. As verified in additional simulations, it is possible to achieve a bandwidth, which is much larger than the measured value.³ Since, at the switched-line phase shifter two pin-diodes per section are forward-biased, the control power amounts to a large level compared to the HCRT device. Therefore, especially when implementing the switched-line phase shifter at phased arrays using many antennas, the power requirement has to be considered in the design of the bias source. In contrast to the HCRT phase shifter the intermodulation distortions are smaller for the switched-line device: The TOI amounts to a 3-dB higher value.

As can be seen in Table 1 the group delay variations within the frequency band of interest are minor for both the switched-line and the HCRT phase shifter. Hence, this parameter is not important for the comparison of the investigated devices. That applies to the response time, too, which is in the order of nanoseconds for both diode types. For example, the used pin-diodes offer a minimal response time⁴ of 0.19 ns.

³If the reference length is chosen carefully, a bandwidth up to one octave is possible for low values of phase shift [1].

⁴which is defined as the i-zone width divided by the saturation velocity

V. CONCLUSION

In this paper two diode-based types of phase shifters were characterised and compared among each other. The first type was the well known switched-line phase shifter using pin-diodes as switching devices. The second type was the hybrid-coupled reflection-type phase shifter using varactor diodes as tunable reactances.

The principle and the implementation were explained for both devices. Important design parameters were highlighted. Especially for the HCRT phase shifter we show that the total phase shift not only depends on the capacitance ratio of the used varactor diode but on the characteristic impedances of additionally used quarter-wavelength transformers as well.

The prepared phase shifters were examined with respect to typical parameters such as insertion loss, input reflection, and third order intercept point. Furthermore the temperature drift of the differential phase shift was determined by measurements using a climatic chamber.

The main focus of this paper was the comparison of the investigated phase shifters. Therefore the quality factor was defined as a parameter for comparison. By using the quality factor different types of phase shifters can be directly compared among each other. The HCRT phase shifter offers the larger quality factor within the frequency band of interest. Furthermore the phase accuracy is not limited by the device itself, because it is an analogue type phase shifter. But that means a digital-analog converter is required, because in phased arrays the phase shift is typically controlled by digital signals. Indeed, the TOI of the HCRT phase shifter is nearly 3 dB smaller compared to the switched-line device, but it is also acceptable for many applications. Especially notable is the low control power of the HCRT phase shifter, therefore it is well suited in large arrays using lots of antennas.

Generally the prepared HCRT phase shifter offers several advantages compared to the switched-line device, making it an attractive alternative for phased array applications. If high phase resolution in association with compact size and low control power is desired, the HCRT phase shifter is well suited. In contrast the switched-line phase shifter allows to control the phase shift by digital signals directly, but a driver circuit is needed anyway.

References

- [1] R. V. Garver, "Broad-Band Diode Phase Shifters," *IEEE Transactions on Microwave Theory and Techniques*, vol. 20, no. 5, pp. 314–323, May 1972.
- [2] S. K. Koul, and B. Bhat, *Microwave and Millimeter Wave Phase Shifters*, Artech House, Boston, 1991.
- [3] J. F. White, "Diode Phase Shifters for Array Antennas," *IEEE Transactions on Microwave Theory and Techniques*, vol. 22, no. 6, pp. 233–242, June 1974.
- [4] R. V. Garver, "360° Varactor Linear Phase Modulator," *IEEE Transactions on Microwave Theory and Techniques*, vol. 17, no. 3, pp. 137–147, March 1969.
- [5] B. T. Hennoch, and P. Tamm, "A 360° Reflection-Type Diode Phase Modulator," *IEEE Transactions on Microwave Theory and Techniques*, corresp., pp. 103–105, January 1971.
- [6] Y. H. Liew, J. Joe, and M. S. Leong, "A Novel 360° Analog Phase Shifter with Linear Voltage Phase Relationship," *Microwave Conference, Asia*, vol. 1, 30 Nov.–3 Dec., 1999.

Authors:

Dipl.-Ing. Mario Schühler
Dipl.-Ing. Christoph Schmidt
Dipl.-Ing. Rainer Wansch
Fraunhofer-Institut Integrierte Schaltungen, Am Wolfsmantel, 33
91058, Erlangen, Germany
Phone: +49 9131 776-6389
Fax: +49 9131 776-359
E-mail: {schuehmo,sit,wan}@iis.fraunhofer.de

Dipl.-Ing. Jörn Weber
Univ.-Prof. Dr. rer. nat. habil. Matthias A. Hein
Technische Universität Ilmenau, Helmholtzplatz, 2
98684, Ilmenau, Germany
Phone: +49 3677 69-1578
Fax: +49 3677 69-1586
E-mail: {joern.weber,matthias.hein}@tu-ilmenau.de